3D Object Recognition by Unmanned Aircraft to Ensure the Safety of Transport Corridors

Rahim Mammadov
dept. Instrumentation engineering
Azerbaijan State Oil and Industry University
Baku, Azerbaijan
rahim1951@mail.ru
ORCID-[0000-0003-4354-3622]

Timur Aliyev
dept. Instrumentation engineering
Azerbaijan State Oil and Industry University
Baku, Azerbaijan
a_tima1@mail.ru
ORCID-[0000-0001-9347-3904]

Gurban Mammadov
Azerbaijan State Scientific-Research Institute for Labor Protection and Occupational Safety
Baku, Azerbaijan
qurban_9492@mail.ru
ORCID-[0000-0002-2874-6221]

***Abstract*—To ensure safety by searching for and identifying suspicious or foreign objects in the area of transport corridors, in this work, it is proposed to use a 3D object recognition system, which is part of an unmanned aviation system. The method of recognition of 3D objects is based on the method of comparison with the standard. In the course of research, the authors obtained a system of equations showing the dependence of the change in the moments of inertia on the angles of rotation of the object image around the abscissa, ordinate and applicate axes. The reference image is formed by rotating through the obtained angles with subsequent direct comparison with the recognized image. If the new image of the template and the object to be recognized are the same, it is concluded that the recognized image corresponds to the template. Thus, after preliminary calculations, the listing of all possible positions is limited to a fixed number of possible positions. To confirm the obtained theoretical results, a computer simulation of the proposed method for recognizing 3D objects was carried out. The experiments were carried out on three images, which are reference images rotated in space at arbitrary angles. The simulation results showed that there is a clear connection between the moments of inertia of a plane figure during its triple rotation in space from the angles of rotation. Taking into account the characteristics of the objects to be recognized and the flight altitude of the unmanned aerial vehicle, it is possible to determine the required distance between them for reliable recognition. This will allow you to correctly build the flight route of the unmanned aerial vehicle and estimate the viewing range. This method can be used to recognize moving ground and air objects.**

Keywords—transport corridors, combating terrorism, 3D object, recognition, reliability, moments of inertia, unmanned aerial vehicle

I. INTRODUCTION

The New Silk Road was officially named by the Chinese as the "Belt and Road Initiative" project, and covers about 70 countries of the Eurasian continent. The concept of the project does not provide for the development of one land and one sea route. Instead, it actually includes the construction of a whole system of transport and economic links in the vast area connecting the Far East and Europe. Project development brings people from all countries along the routes together in a collaborative effort for common development and benefit-sharing through win-win cooperation [1, 2, 3].

In parallel, the "Program of Central Asian Regional Economic Cooperation" is actively developing. The partnership between China, the countries of Central Asia and the Caucasus stimulates the development of transport and energy and also facilitates trade in the vast territory of Eurasia [4].

Within the trans-Eurasian corridor connecting East Asia and Western Europe, the South Caucasus can be considered a central hub. Infrastructure projects such as the Baku-Tbilisi-Kars railway highlight the importance of this route. In addition, the delivery of goods from China and Asian countries to Europe via the Caspian Sea is a short and convenient way. Given the geographical location of the current economic development, Azerbaijan can be considered a focal point for both transnational exchange of goods and tourism projects [5, 6].

II. PROBLEM STATEMENT

Terrorism is not a new phenomenon. Many countries in Europe, Latin America, Africa and Asia have faced terrorist movements of all kinds, united by a willingness to use violence against innocent civilians to achieve their goals. Terrorists often use explosive devices as one of the most common weapons. Information on making explosive devices is readily available in books and other sources. The materials needed for the explosive device can be found in many places, including various home appliance and auto parts stores. The vast majority of attacks are carried out by individuals acting alone - often with limited training and readily available weapons - targeting densely populated or highly symbolic locations [7, 8, 9].

Currently, there are a large number of measures to prevent this kind of threat [10, 11]. However, the rapid development of technology at the end of the 20th century and the beginning of the 21st century, as well as the globalization of the economy, contributed to the emergence of highly organized terrorist groups ready to sacrifice thousands of lives to achieve their goals (for example, the attack on the World Trade Center on September 11 in New York). At the same time, the risk of mega-terrorism has become quite real, and the transport system has gained great importance in the eyes of security services around the world as the main target and / or a means for future attacks [12]. The development of high technologies has made it possible to reduce prices for sophisticated equipment, and the globalization of the "black market" has given even medium-sized terrorist organizations

the opportunity to buy a combat drone, given that its price is comparable to the price of a car [13]. In addition, training for a participant in an organization to control a combat aircraft or vehicle has become available.

The rates are extremely high, as any major disruption to the transport system could cause significant damage to the country's economy and reduce its reputation in the world.

At present, sufficiently effective tools have been developed to protect marine corridors [14]. However, works are worse for land transport corridors. The location of the corridor in sparsely populated or hard-to-reach areas makes it difficult to ensure its safety. This is due to the fact that a combat aircraft can quickly enough and (using the terrain) imperceptibly approach, strike and hide.

Thus, we can say that ensuring the security of its transport corridors is and will be one of the main tasks of the national security of each country.

III. PROBLEM SOLVING

Drone is an informal name for devices known as unmanned aerial vehicles (UAV), unmanned aircraft systems (UAS), and small unmanned aircraft systems (sUAS). The term UAS refers to the entire system for using a drone, including the aircraft and the ground control unit, while UAV refers only to the vehicle itself [15].

Drone opportunities can be found in almost all fields of life. One of the directions in the civil sector is the use of UAS to prevent various types of crimes and terrorist acts [16].

The use of drones to automate routine and monotonous work can improve safety performance, reduce risks, and improve quality. It will also free people to focus on more responsible, interesting and rewarding work [17].

Fig. 1. presents a generalized block diagram of the UAS [18]. The standard set of equipment used in most UAS includes: a transmitter for controlling the UAV (Tr); the UAV itself, consisting of a control signal receiver and the transmitter of useful information (Re+Tr), a flight computer (FC), a navigation system (NS+GPS), a sensor unit (SU) and a camera for photo and video shooting; a ground control station (GCS) for semi-autonomous control and processing of the received information.

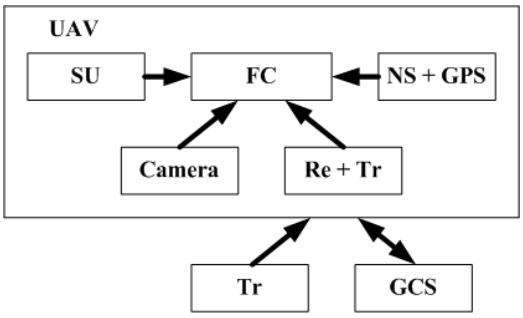

Fig. 1. UAS block diagram

To ensure safety, by searching and identifying suspicious or foreign objects in the area of transport corridors, this work proposes the use of a system for recognizing 3D objects. With the help of the organ of vision of the system (a camera located on a high-flying UAV), we obtain a two-dimensional image of the earth's surface. This image will also contain objects located at a low height. Further, this information will be transmitted to the ground for further processing.

Due to the fact that the object of interest (OI) in most cases will be away from the UAV (Fig. 2), its image will undergo such distortions as rotation and shift. As a result, all geometric features will be strongly distorted and recognition by geometric features becomes much more difficult.

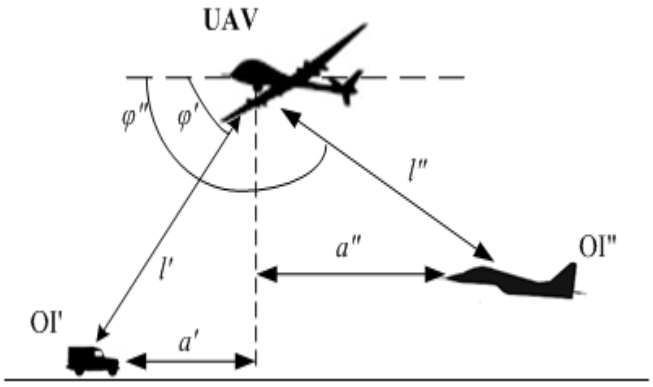

Fig. 2. The relative position of objects of interest relative to the UAV.

Currently, many techniques have been developed for the recognition of spatial images of objects, however, each of them has its own drawbacks. So in [19], parallel transfer and rotation of the image is considered, which is a special case of spatial displacements. In [20, 21], the analysis is carried out by reference points, the numbering of which should remain constant with spatial distortions, which is not always achievable. In [22, 23], the analysis of the image is carried out along the contour, which is the most sensitive to distorting factors. In [24], the moments of inertia are considered as the main features, however, the analysis of the properties of the moments of inertia showed that the moments of inertia, as features, are quite integral for a wide range of objects. This makes it difficult to recognize objects of the same cluster.

In this paper, it is proposed to use statistical moments as image landmarks, and based on this principle, develop an effective method for recognizing 3D objects.

One of the ways to recognize an object located in an arbitrary way in space is to recognize its sides from two-dimensional images by comparing them with reference images.

In fact, the image of the side of an object is a flat closed single-line or multi-line figure. The process of recognizing an object located arbitrarily in space can be reduced to recognizing several flat figures located arbitrarily in space. Because a flat figure is a solid body, then the analysis of its position in space can be performed by analyzing the position of a fixed marker point located on a flat figure. In this case, an arbitrary location of a plane figure, and therefore a marker point in space, is considered as rotations of a plane figure around three coordinate axes. The analysis of the position of a flat figure will be carried out by analyzing the position of the projection of the marker point on the frontal plane. In this case, the origin point is located in the center of the flat figure.

In the course of research [25], the authors obtained the dependence of the change in the coordinates of the projection of the marker point when the frontal plane rotates around the horizontal axis OX, followed by rotation around the vertical axis OY:

$$x_2 = x_0 \cdot \cos\beta, \qquad (1)$$

$$y_2 = y_0 \cdot \cos\alpha \pm x_0 \cdot \sin\beta \cdot \sin\alpha, \qquad (2)$$

Where x_0, y_0 – are the coordinates of the marker point on the original frontal plane, x_2, y_2 – are the coordinates of the marker longing after its double rotation, α – is the angle of rotation around the horizontal axis, β – is the angle of rotation around the vertical axis.

After integrating expressions (1) and (2) for the entire figure, we obtain expressions for the moments of inertia of a flat figure after its double rotation in space:

$$J_{X2} = \cos^3\alpha\cdot\cos\beta\cdot J_{X0} \pm 2\cdot\cos^2\alpha\cdot\sin\alpha\cdot\sin\beta\cdot\cos\beta\cdot J_{X0Y0} +$$

$$+\cos\alpha\cdot\sin^2\alpha\cdot\cos\beta\cdot\sin^2\beta\cdot J_{Y0}, \quad (3)$$

$$J_{Y2} = \cos\alpha\cdot\cos^3\beta\cdot J_{Y0}, \quad (4)$$

$$J_{X2Y2} = \cos^2\alpha\cdot\cos^2\beta\cdot J_{X0Y0} \pm \cos\alpha\cdot\sin\alpha\cdot\cos^2\beta\cdot\sin\beta\cdot J_{Y0}, \quad (5)$$

Where J_{X0}, J_{Y0}, J_{X0Y0} – respectively the moment of inertia of the original figure along the OX axis, along the OY axis and the centrifugal moment of inertia; J_{X2}, J_{Y2}, J_{X2Y2} – respectively, the moment of inertia of a flat figure, after its double rotation in space, along the OX axis, along the OY axis and the centrifugal moment of inertia.

As is known [20], the moments of inertia of the section when the axes passing in the section plane are rotated around the axis passing perpendicular to the section plane are related by equations (6) ÷ (8):

$$J_U = J_X\cdot\cos^2\gamma + J_Y\cdot\sin^2\gamma - J_{XY}\cdot\sin 2\gamma, \quad (6)$$

$$J_V = J_X\cdot\sin^2\gamma + J_Y\cdot\cos^2\gamma + J_{XY}\cdot\sin 2\gamma, \quad (7)$$

$$J_{UV} = J_{XY}\cdot\cos 2\gamma + \frac{J_X - J_Y}{2}\cdot\sin 2\gamma, \quad (8)$$

Where J_X, J_Y, J_{XY}– axial and centrifugal moments of inertia of the section relative to the original axes; J_U, J_V, J_{UV} – axial and centrifugal moments of inertia of the section relative to the rotated axes; γ – angle of rotation.

Substituting expressions (3) ÷ (5) into equations (6) ÷ (8) and denoting the constants J_U, J_V, J_{UV}, respectively, as J_{X3}, J_{Y3} and J_{X3Y3}, we obtain the dependence of the change in the moments of inertia of a plane figure during its triple rotation in space:

$$J_{X3} = f(\alpha, \beta, \gamma, J_{X0}, J_{Y0}, J_{X0Y0}), \quad (9)$$

$$J_{Y3} = f(\alpha, \beta, \gamma, J_{X0}, J_{Y0}, J_{X0Y0}), \quad (10)$$

$$J_{X3Y3} = f(\alpha, \beta, \gamma, J_{X0}, J_{Y0}, J_{X0Y0}), \quad (11)$$

By solving the system of equations (9) ÷ (11), expressions for the variables α, β and γ are determined.

Recognition is carried out in three stages:

- At the first stage, the reference image of the object is rotated by the calculated angles α, β, γ. U- turns are made in the following sequence: at the beginning, a turn around the center of mass by an angle γ; further rotation around the abscissa axis by an angle α (in this case, the ordinate axis will rotate along with the image); and at the end, a turn around the rotated ordinate by an angle β.

- At the second stage, the scale is adjusted. Using an on-board ranging instrument (laser or radio rangefinder), the distance to the object of interest *l* is determined *(fig. 2)*. Based on the distance, the change in the scale of the object's image is calculated. In the absence of rangefinders, the scale can be determined using the navigation system. The distance is determined indirectly from two images taken at different points in space. Knowing the exact location of the UAV in space, by the value of the angle between the longitudinal axis and the direction of the camera φ *(fig. 2)*. From two images, you can calculate the distance to the object of interest, and therefore the scale.

- At the third stage, a direct comparison of the resulting image with the recognizable. For this, the center of mass of the recognized image is reduced to the center of mass of the converted reference image.

If in any of the new positions of the reference images coincide, then it is concluded that the recognized image corresponds to the reference. In this case, the quantities α, β and γ determine the orientation of the object in space.

That is, after preliminary calculations, the enumeration of all possible positions is limited to a fixed number of possible positions.

However, there will be no complete coincidence of the images due to the presence of sampling distortion in the converted image. This manifests itself on its contour in the form of a change in the values of individual pixels. As a numerical estimate of the similarity between the reference and the recognized image, you can use the transformed measure of the Manhattan distance [26]:

$$Z = \sum_{i=1}^{m} |A(x,y)_i - B(x,y)_i| \le \varepsilon = 2\cdot P \quad (12)$$

Where: A (x, y) and B (x, y) - respectively the values of points belonging to the standard and the recognized image; x, y – pixel coordinates in the image; *i* – the number of pixels in the image; ε – the value of the confidence threshold depending on the size of the images and the computational error of the analysis; P – reference perimeter.

This measure shows the discrepancy between the images, i.e. number of mismatched pixels in direct comparison.

If the discrepancy for any image does not exceed the permissible deviation, then it is concluded that the image under consideration corresponds to the reference image, and the object is oriented in space in accordance with α, β and γ.

IV. Computer simulations

To check the obtained theoretical results, computer simulation was carried out.

The proposed technique was investigated using images of objects of the same nature. The ability to fly and carry any combat load was taken as this character. For example, the MiG-25, SU-25 and SU-30 aircraft were taken.

In fig. 3 shows three flat figures, which are horizontal projections of these objects. These images can theoretically be acquired by a high-flying UAV that continuously probes the earth's surface. These images are entered into the ground control station (GCS) database, where recognition is performed, as reference objects.

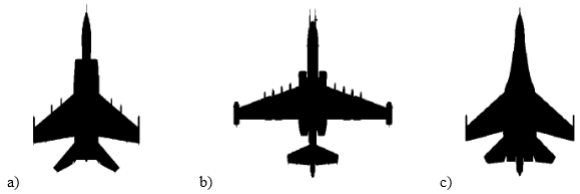

Fig. 3. Images from the database:

a – MIG-25; b – SU-25; c – SU-30

As a characteristic for determining the difference in the images of objects, one can take the "shape index" ρ [27]:

$$\rho = \frac{\text{Perimeter}^2}{Area}. \quad (13)$$

For a more detailed study, several options for images of the proposed objects were considered, differing in size. Table 1 summarizes the main parameters of the considered images.

Table 1. Reference image parameters

Image	Object height, pixel	Object width, pixel	Object area, pixel	Object shape index, (ρ).
Fig. 1, a.	300	190	18646	107
	350	222	25370	
	400	253	32995	
	450	285	41910	
	500	317	51768	
Fig. 1, b.	300	284	20119	153
	350	331	27292	
	400	379	35464	
	450	426	44712	
	500	473	55437	
Fig. 1, c.	300	194	19766	93
	350	226	26772	
	400	258	34794	
	450	291	44113	
	500	323	54378	

The object of interest can be in four positions relative to the UAV:

1. The object of interest is located directly under the UAV. In this case, we can say that the camera with which the image was obtained is directed perpendicularly downward.

2. The object of interest is located away from the UAV, while the image of the longitudinal axis of the object is parallel or coincides with the longitudinal axis of the UAV.

3. The object of interest is located away from the UAV, while the image of the longitudinal spine of the object is perpendicular to the longitudinal axis of the UAV.

4. The object of interest is located away from the UAV and its position is random.

To obtain a set of images for the first position, the reference images were rotated around the center of mass by angles γ with a step of 40º (40º; 80º; 120º; 160º; 200º; 240º; 280º; 320º). As a result, 8 transformed images were obtained for each size of each shape. The obtained images were used to determine the axial (J_{Xfig}, J_{Yfig}) and centrifugal (J_{XYfig}) moments.

Also, according to formulas (9) ÷ (11) for these images, the moments of inertia J_{X3}, J_{Y3}, J_{X3Y3} were calculated. Considering that the image made only one rotation, the variables α and β during the calculations were equal to 0.

To obtain a set of images for the second position, the reference images were rotated around the abscissa axis by angles α with a step of 10º (10º; 20º; 30º; 40º; 50º; 60º; 70º; 80º). As a result, 8 transformed images were obtained for each size of each shape. The obtained images were used to determine the axial (J_{Xfig}, J_{Yfig}) and centrifugal (J_{XYfig}) moments.

Also, according to formulas (9) ÷ (11) for these images, the moments of inertia J_{X3}, J_{Y3}, J_{X3Y3} were calculated. Taking into account that the image made only one rotation, the variables β and γ in the course of calculations were equal to 0.

To obtain a set of images for the third position, the reference images were rotated around the ordinate by angles β with a step of 10º (10º; 20º; 30º; 40º; 50º; 60º; 70º; 80ºAs a result, 8 transformed images were obtained for each size of each shape. The obtained images were used to determine the axial (J_{Xfig}, J_{Yfig}) and centrifugal (J_{XYfig}) moments.

Also, according to formulas (9) ÷ (11) for these images, the moments of inertia J_{X3}, J_{Y3}, J_{X3Y3} were calculated. Taking into account that the image made only one rotation, the variables α and γ during the calculations were equal to 0.

To obtain a set of images for the fourth position, the reference images were rotated around the center of mass at angles γ with a step equal to 40°, followed by turns around the horizontal axis at angles α with a step equal to 10 ° and around the vertical axis at angles β with a step equal to 10º (10º,10º,40º; 20º,20º,80º; 30º,30º,120º; 40º,40º,160º; 50º,50º,200º; 60º,60º,240º; 70º,70º,280º; 80º,80º,320º). As a result, 8 transformed images were obtained for each size of each shape. The obtained images were used to determine the axial (J_{Xfig}, J_{Yfig}) and centrifugal (J_{XYfig}) moments. Also, according to formulas (9) ÷ (11) for these images, the moments of inertia J_{X3}, J_{Y3}, J_{X3Y3} were calculated.

Further, the absolute discrepancies Δ were calculated between the corresponding moments of inertia obtained from the images and by the formulas (9) ÷ (11):

$$\Delta_X = |J_{Xfig} - J_{X3}|, \quad \Delta_Y = |J_{Yfig} - J_{Y3}|, \quad \Delta_{XY} = |J_{XYfig} - J_{X3Y3}|. \quad (14)$$

In fig. 4 shows the averaged changes in the absolute discrepancy ΔX (fig. 4, a), ΔY (fig. 4, b) and ΔXY (fig. 4, c) for the object shown in fig. 3, a.

a)

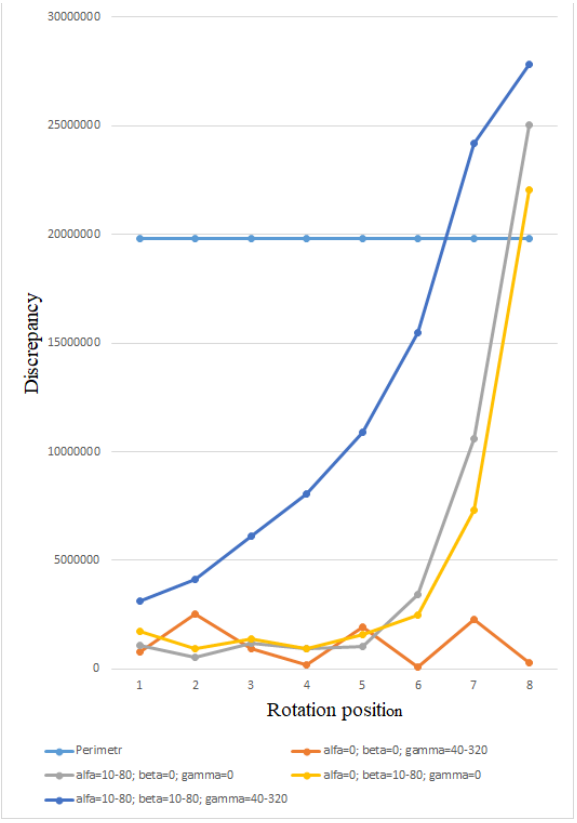

b)

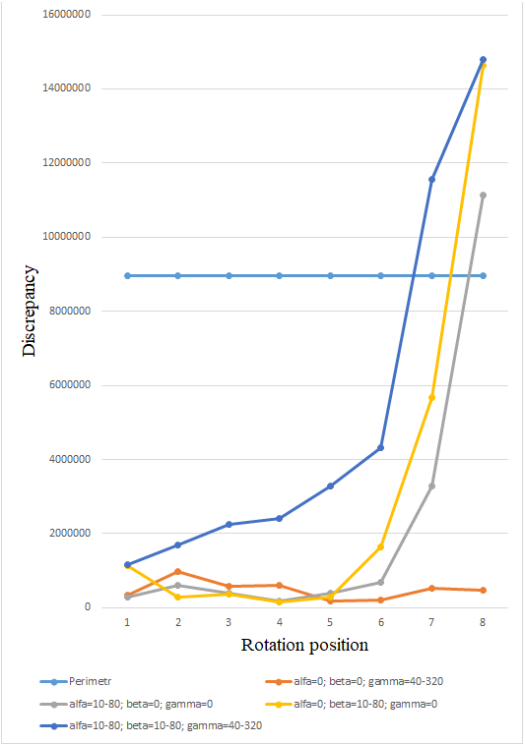

c)

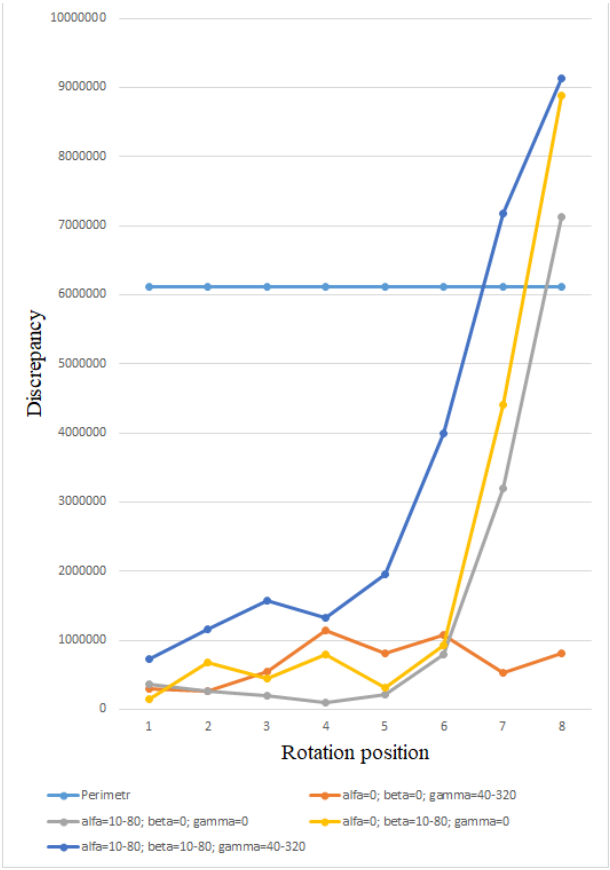

Fig. 4. Average changes in the absolute discrepancy in the moments of inertia for the image of the MIG-25 aircraft.

In fig. 5 shows the averaged changes in the absolute discrepancy ΔX (fig. 5, a), ΔY (fig. 5, b) and ΔXY (fig. 5, c) for the object shown in fig. 3, b.

a)

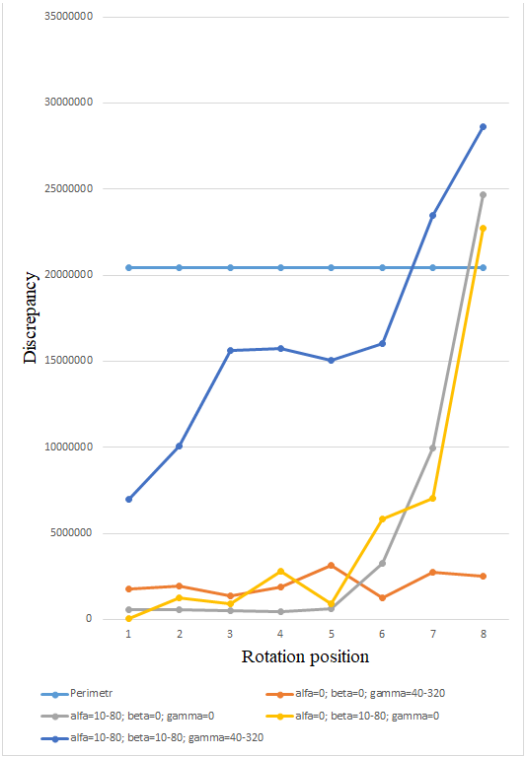

b)

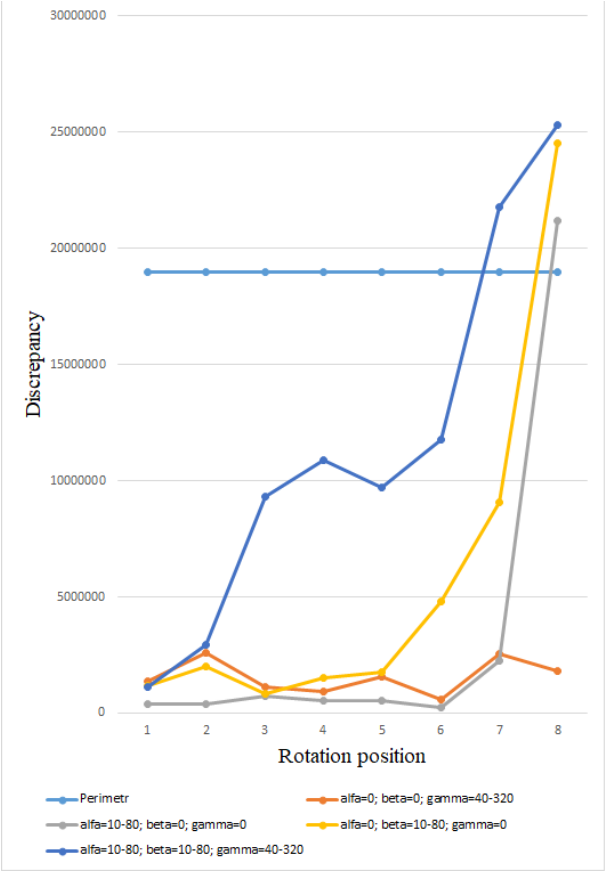

c)

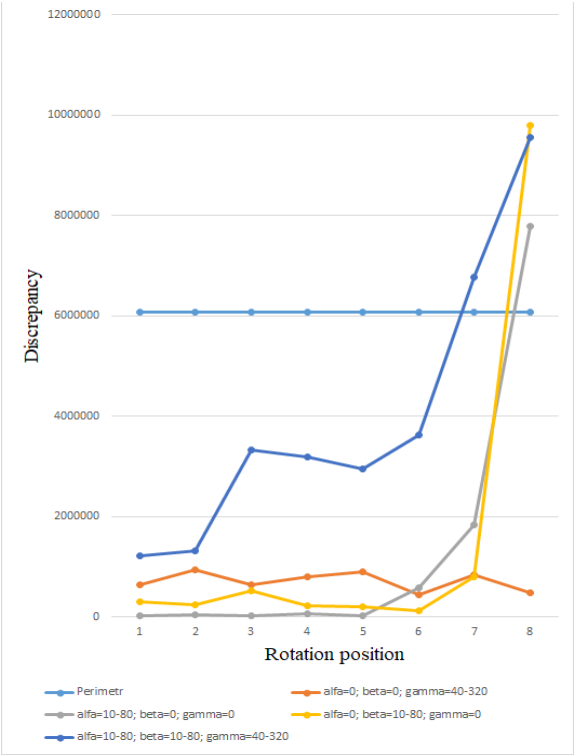

Fig. 5. Average changes in the absolute discrepancy in the moments of inertia for the SU-25 aircraft image.

In fig. 6 shows the averaged changes in the absolute discrepancy ΔX (fig. 6, a), ΔY (fig. 6, b) and ΔXY (fig. 6, c) for the object shown in fig. 3, c.

a)

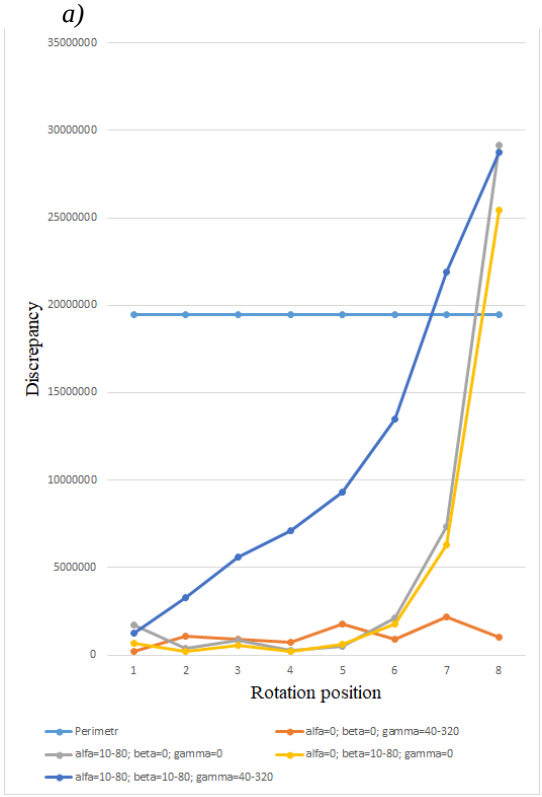

b)

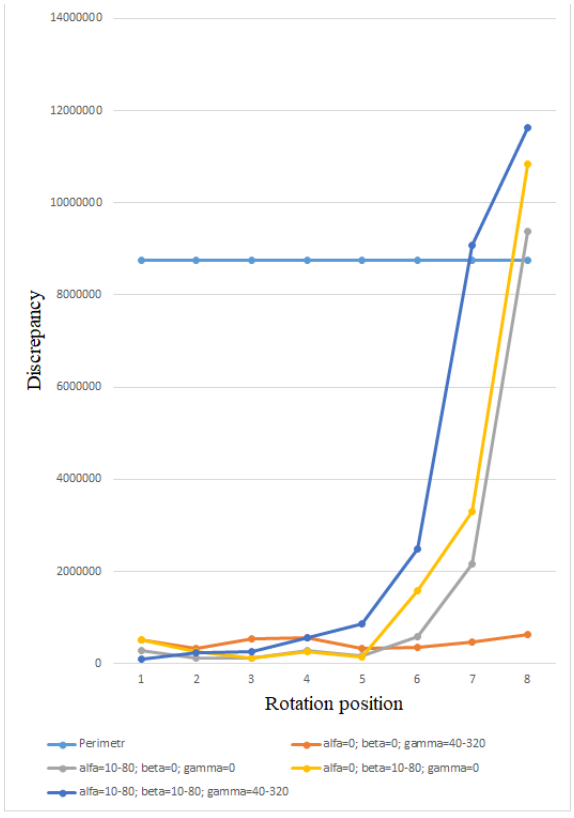

c)

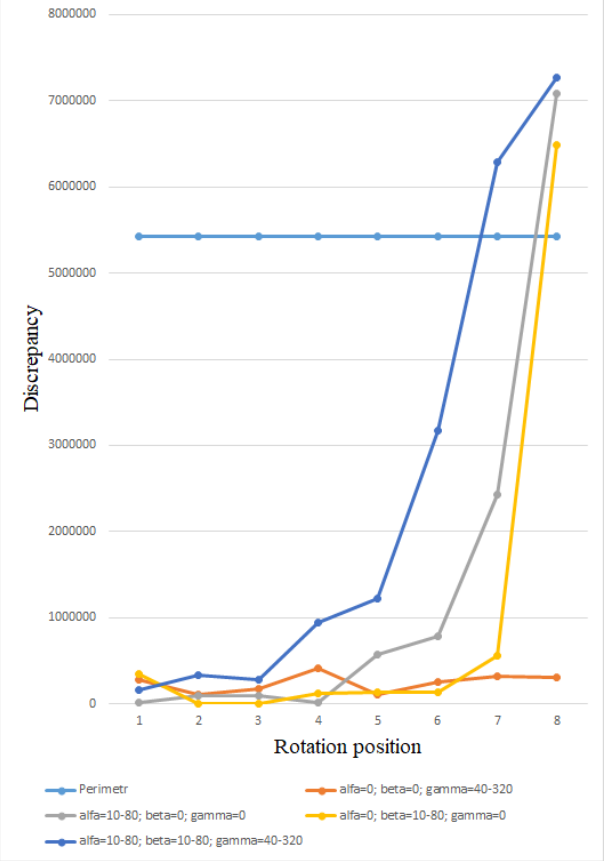

Fig. 6. Average changes in the absolute discrepancy in the moments of inertia for the SU-30 aircraft image.

For simplicity, the evaluation of the effectiveness of the proposals of the method was carried out according to the values of Δ. That is, if the value of Δ does not exceed the threshold value, then the recognition can be considered reliable. Since the perimeter of the object is the most sensitive to any image transformations, the corresponding moment of inertia of the perimeter was chosen as the threshold value.

V. CONCLUSİON

The analysis of the change in the moments of inertia of a plane figure during its rotation around three coordinate axes for recognition carried out by the authors showed that there is a clear relationship between the moments of inertia of a plane figure during its triple rotation in space on the angles of rotation.

Analyzing Fig. 4, fig. 5 and fig. 6, it can be assumed that: the law of variation of Δ is close to an increasing exponential, when there is rotation around the abscissa and / or ordinate axis; and the law of variation of Δ is close to harmonic oscillation when there is rotation only around the center of mass.

Further analysis shows that if the recognized image has α = 0 and β = 0, then for any value of γ the recognition will have a high reliability. Thus, we can say that this rotation has a minimal effect on the recognition process, and the discrepancy is mainly due to the computational error.

With an increase in α or β, with the exception of the limit values (more than 80^0), the recognition will have an acceptable reliability. With a simultaneous increase in α and β, high reliability will be at angles up to 40^0, and at angles more than 60^0, the recognition reliability will be low. This may be due to a decrease in the image area of the object of interest. Studies have shown that the larger the image area of the object, the higher the recognition reliability. However, increasing the area greatly slows down the recognition process, and powerful computing resources are required to implement it.

In addition, the shape index also affects the recognition reliability. As can be seen from Fig. 5, for objects with a high shape index, high reliability can be obtained only at small angles of image rotation (less than 20^0).

Taking into account the shape index of the objects of interest and the UAV flight altitude, it is possible to determine the required distance a (Fig. 2). This will allow you to correctly plot the UAV flight route and estimate the viewing range. This technique can also be applied to the recognition of moving ground objects.

REFERENCES

[1] Zoran Wittine , Hrvoje Josic and Antea Barisic. Analysis Of Characteristics And Potential Effects Of The New Silk Road Initiative // Conference of the International Journal of Arts & Sciences, ISSN: 1943-6114 :: 11(02):255–260 (2018).

[2] Aleksandar Janković. New Silk Road – New Growth Engine // The Review of International Affairs, Belgrade, vol. LXVII, No. 1161, (2016)

[3] New Stories of the Silk Road. No. 9, (2017)

[4] The New Silk Road. Ten Years of the Central Asia Regional Economic Cooperation Program. Mandaluyong City, Philippines: Asian Development Bank, (2011).

[5] Schuhbert, A., & Thees, H. Of routes and corridors: Challenges and opportunities for Silk Road destinations in the southern Caucasus. Journal of Tourism, Heritage & Services Marketing, 6(2),pp. 21-29, (2020).

[6] Tamila Sh. Khalilova, Renying Li, Elchin N. Khalilov. Caspian Route Of The Silk Road // International Journal of Asian History, Culture and Tradition6 Vol.4, No.4, pp.1-9, (2017)

[7] Daniel O'Donnell. International Treaties Against Terrorism And The Use Of Terrorism During Armed Conflict And By Armed Forces // International Review of the Red Cross, Vol. 88, No 864, (2006)

[8] www.fema.gov/pdf/areyouready/terrorism.pdf.

[9] Communication From the Commission to the European Parliament, the European Council, the Council, the European Economic and Social Committee and the Committee of the Regions. A Counter-Terrorism Agenda for the EU: Anticipate, Prevent, Protect, Respond, (2020).

[10] Center for the Protection of National Infrastructure. Protecting Against Terrorism, (2010).

[11] United Kingdom Country Security Report, (2021).

[12] Organisation for Economic Co-operation and Development. Security in Martime Transport: Risk Factors and Economic Impact. Maritime Transport Committee, (2003).

[13] Ricardo Valerdi. Cost Metrics for Unmanned Aerial Vehicles // Collection of Technical Papers - InfoTech at Aerospace: Advancing Contemporary Aerospace Technologies and Their Integration. Vol. 3, pp. 1753 – 1758, (2005)

[14] NATO Public Diplomacy Division. Briefing. Combating terrorism at sea, (2008)

[15] Police Executive Research Forum. Drones: A Report on the Use of Drones by Public Safety Agencies—and a Wake-Up Call about the Threat of Malicious Drone Attacks. Washington, DC: Office of Community Oriented Policing Services, (2020).

[16] Bart Custers. The Future of Drone Use. Opportunities and Threats from Ethical and Legal Perspectives // Information Technology and Law Series, Vol. 27, (2016)

[17] PwC. Skies without limits. Drones - taking the UK's economy to new heights, (2018)

[18] Mitch Campion, Prakash Ranganathan, and Saleh Faruque. A Review and Future Directions of UAV Swarm Communication Architectures // IEEE International Conference on Electro/Information Technology, (2018)

[19] Мамедов Р.К., Муталлимова А.С., Алиев Т.Ч., Использование моментов инерции изображения для инвариантного к аффинным преобразованиям распознавания// Восточно-Европейский журнал передовых технологий. №4/3 (58), 2012, с. 4-7.

[20] Vimal Sudhakar Bodke, Omkar S Vaidya (2017). Object Recognition in a Cluttered Scene using Point Feature Matching. *International Journal for Research in Applied Science & Engineering Technology*, 286-290.

[21] Toshiaki Ejima, Shuichi Enokida, Toshiyuki Kouno (2014). 3D Object Recognition based on the Reference Point Ensemble. *International Conference on Computer Vision Theory and Applications*, 261-269.

[22] Farnoosh Ghadiri, Robert Bergevin, Guillaume-Alexandre Bilodeau: Carried Object Detection Based on an Ensemble of Contour Exemplars. 14th European Conference Computer Vision – ECCV 2016. Amsterdam, October 11–14, pp. 852-866 (2016).

[23] Xin Li, Fan Yang, Hong Cheng, Wei Liu, Dinggang Shen: Contour Knowledge Transfer for Salient Object Detection. 15th European Conference Computer Vision – ECCV 2018. Munich, September 8-14, pp. 370-385 (2018).

[24] Mohammad Arafah, Qusay Abu Moghli (2017). Efficient Image Recognition Technique Using Invariant Moments and Principle Component Analysis. Journal of Data Analysis and Information Processing, 1-10.

[25] Мамедов Р.К., Алиев Т.Ч. Контроль положения 3D-объектов в гибких автоматизированных системах. Повышение достоверности распознавания. – LAP LAMBERT academic publishing, 2016. - 90 с.

[26] Mammadov R.G., Aliyev T.Ch., Mutallimova A.S. Identification of spatial objects by their monochrome images of autonomous mobile robots // International journal of engineering research and science», vol.2, №11, November 2016, India, pp.125-128.

[27] Jens Feder. Fractals. Plenum press. New York. 1988